ELSEVIER

Cement & Concrete Composites 24 (2002) 491–496

Cement & Concrete Composites

www.elsevier.com/locate/cemconcomp

Non-linear finite element analyses of punching shear failure of column footings

Mikael Hallgren *, Mats Bjerke

Scandiaconsult, P.O. Box 4205, SE-102 65 Stockholm, Sweden

Abstract

Current design methods and code formulas for the assessment of the punching shear strength are normally based on tests on slabs with relatively high slenderness, i.e., with high shear-span to depth ratios. Column footings normally have low shear-span to depth ratios. Previous punching tests on column footings indicate that the failure mechanism for punching of slabs with low shear-span to depth ratios differs from that of slabs with high shear-span to depth ratios. In this investigation, punching tests on two circular column footings of reinforced concrete were simulated numerically. The results show how the failure mechanism differs from that of more slender slabs. A parametric study also confirms that the punching shear strength of the analysed slabs strongly depends on the compressive strength of concrete.

Keywords: Punching; RC slabs; Column footings; FE-analyses

1. Introduction

Current models and codes formulas for the assessment of the punching shear strength are based on tests on relatively slender slabs with shear-span to depth ratios of more than 3–4. Column footings have usually much smaller values of the shear-span to depth ratio. The structural behaviour of footings loaded to punching shear failure is not clear.

The previous investigations by Dieterle [1], and also a more recent investigation by Hallgren et al. [2], indicate that the mechanism of punching shear failure of column footings differ from that of more slender slabs. The tests reported in [2] show that the angle of the punching shear crack is much steeper in column footings with low shear-span to depth ratios than observed in previous tests on more slender slabs. Furthermore, the compressive strength of concrete had a stronger influence on the punching shear strength of column footings than observed in previous tests on slender slabs, see Fig. 1.

Theoretical research work for the development of a relevant method for the design of column footings is needed. The finite element method, using a non-linear approach where the cracking of concrete is considered, appears to be a good tool for this work.

The present paper is based on the diploma-work [3] of the second author and supervised by the first author. In the investigation, the failure mechanism for punching of column footings was studied by numerical simulations of previous punching shear tests [2]. The numerical simulations were made using the non-linear finite element method for reinforced concrete based on the smeared crack approach. The results from the numerical simulations are compared with the results from the previous tests. Furthermore, a parametric study is presented where the influences of geometrical and material properties on the computed load and deformation capacities are shown.

2. Punching shear tests on column footings

Fourteen column footings of reinforced concrete were tested previously [2]. Two of them were circular in shape, while the others were quadratic. Due to polar symmetry of the circular slab, they were chosen for the axi-symmetric FE-modelling presented in this paper. The measured properties of the two slabs are given in Table 1.

* Corresponding author. Tel.: +46-8-615-60-00; fax: +46-8-702-19-21.
E-mail address: mhnbos@scc.se (M. Hallgren).

0958-9465/02/$ - see front matter
PII: S0958-9465(01)00065-8

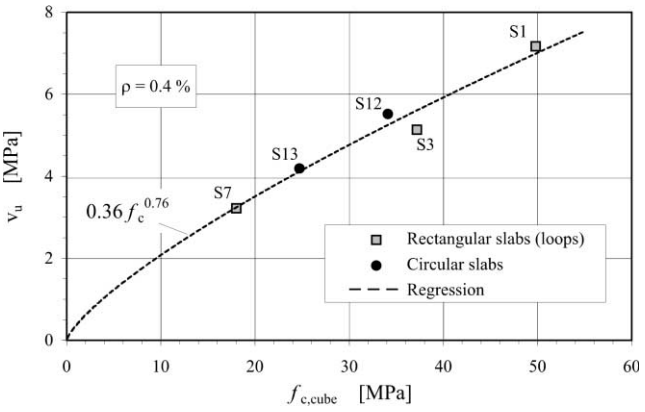

Fig. 1. Punching shear strength v_u as function of the compressive cube strength $f_{c,cube}$ [2].

The geometry of the slabs is shown in Fig. 2. The slabs were two-way reinforced with ∅8 mm deformed bars, see Fig. 3. The slabs were tested upside down, as shown in Fig. 4. The load was provided by a hydraulic jack placed under the column stub. The slab was held back by 12 tie rods placed along a circle with diameter 674 mm, which was approximated to be the support line equivalent to the effect of a uniform surface support of e.g., soil. This approximation was verified in [2] by additional test on slabs with uniform surface loads applied by a series of smaller hydraulic jacks.

The tests indicated that the compressive strength of concrete had a strong influence on the punching shear strength of the column footings. The punching shear strength increased with the compressive strength at a higher rate than derived in other investigations based on tests on more slender slabs with higher shear-span to depth ratios [6].

Furthermore, the angle of the punching shear cracks observed in the tests of the column footings was about 50–60°, see Fig. 5, which is much steeper than the shear-crack slopes of about 30–40° observed in previous tests on more slender slabs [6].

3. Finite element analyses

3.1. General

The FE-analyses were performed with the special-purpose computer program SBETAX 1.2 [4], which is

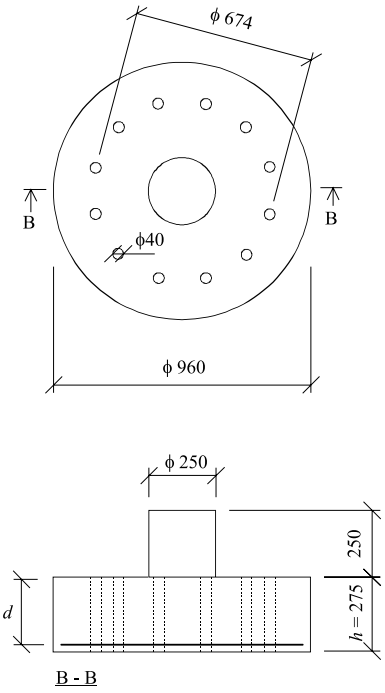

Fig. 2. Dimensions of the slabs [2]. Measurements in mm.

developed for the analyses with axi-symmetric FE-models. SBETAX is based on SBETA [5], which is used for the non-linear analyses of reinforced concrete structures modelled in 2D. The smeared crack approach for modelling of cracks is adopted in SBETA.

3.2. Material models

The constitutive material models used in the analyses are shown in Fig. 6. In order to avoid any stress locking phenomenon in the shear cracks, a rotated-crack model was chosen, see Fig. 6(c). The failure model for concrete is based on non-linear fracture mechanics. In this model, the softening behaviour of concrete after cracking is controlled by tensile strength R_t and fracture energy G_f, see Fig. 5(d). R_t, G_f and the modulus of elasticity E_c were approximated according to MC90 [8].

3.3. Slab model

Benefiting from the polar symmetry of the geometry of the slab, half the cross-section of the slab was modelled with isoparametric elements defined in 2D with

Table 1
Measured properties of the slabs

Slab no.	Slab height, h (mm)	Effective depth, d (mm)	Concrete strength, $f_{c,cube}$ (MPa)	Yield stress of reinforcement, f_{sy} (MPa)	Reinforcement ratio, ρ ($\times 10^{-2}$)	Ultimate load, P_u (kN)
S12	275	242	34.1	621	0.42	1049
S13	275	244	24.7	621	0.42	803

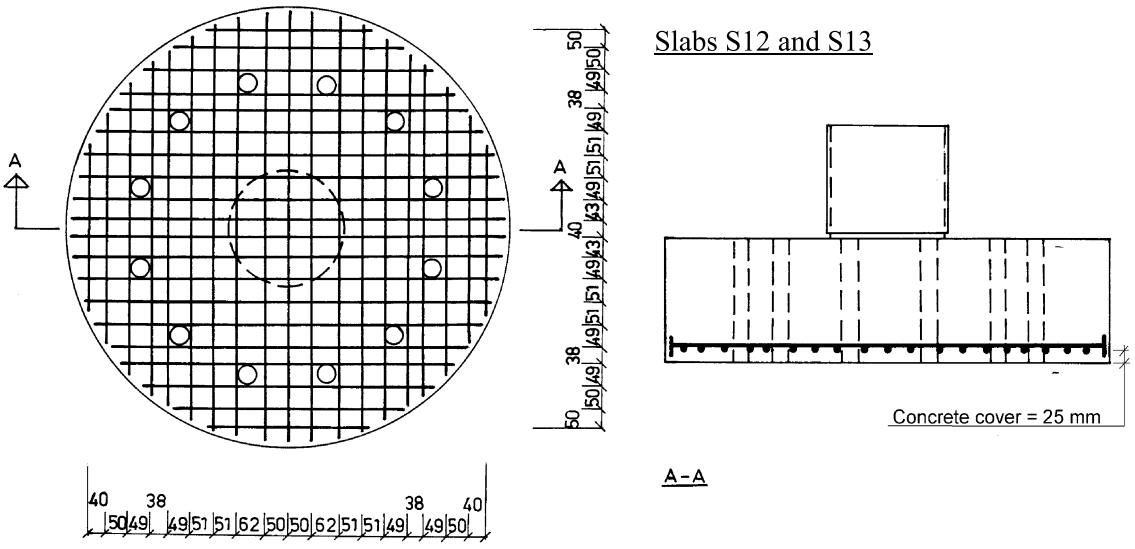

Fig. 3. Reinforcement of the slabs [2]. Measurements in mm.

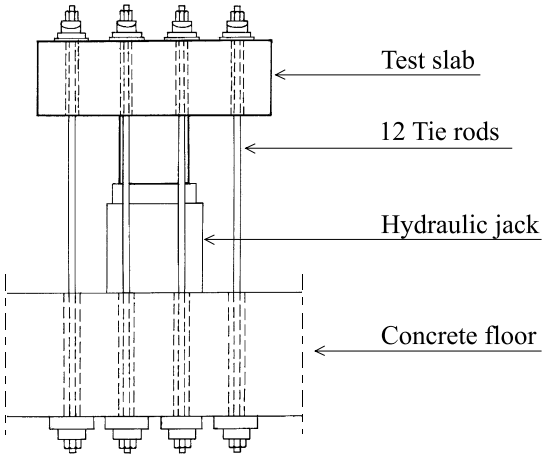

Fig. 4. Test set-up [2].

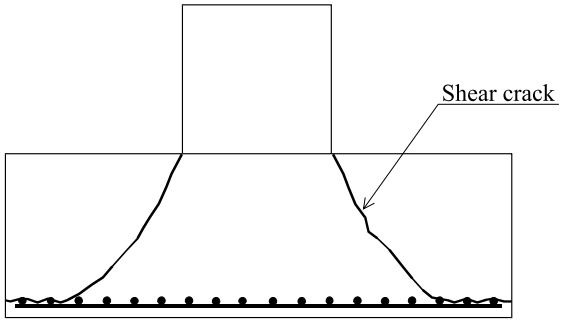

Fig. 5. Typical profile of the failure surface [2].

four nodes each. The model consisted of 456 elements, see Fig. 7(a). The axi-symmetric model was generated by giving the nodes additional degrees of freedom in the out-of-plane direction with reference to the line of symmetry along the left-hand side of the model. The reinforcement was smeared in a band of elements as shown in Fig. 7(b).

In the non-linear FE-analyses, the load was increased deformation controlled in steps according to the Newton–Raphson iteration method with line search.

4. Results

Fig. 8 shows the load–deflection curves derived from the FE-analyses of the two slabs. The computed

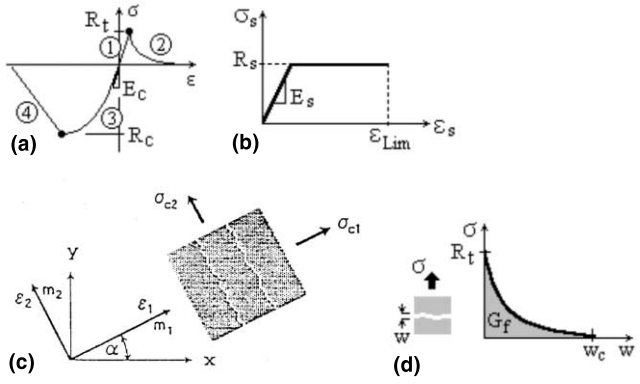

Fig. 6. The material models used in the FE-analyses [4]. R_t is the concrete tensile strength, R_c is the concrete compressive strength, E_c is the concrete modulus of elasticity, R_s is the steel tensile strength, E_s is the steel modulus of elasticity, m_1 and m_2 are the material axes, ε_1 and ε_2 are the principal strain axes, G_f is the concrete fracture energy and w is the crack width. (a) Stress–strain model for concrete. (b) Stress–strain model for steel. (c) Rotated-crack model. (d) Post-cracking softening model.

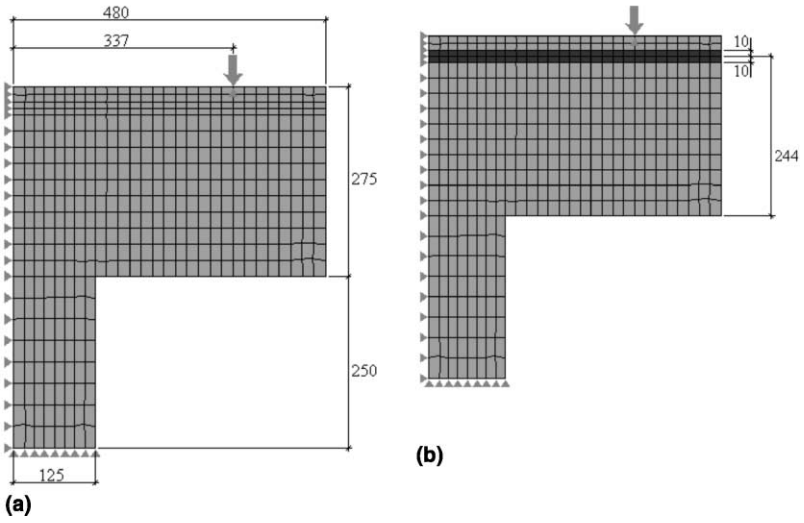

Fig. 7. The slab model. Measurements in mm. (a) Dimensions. (b) Reinforcement.

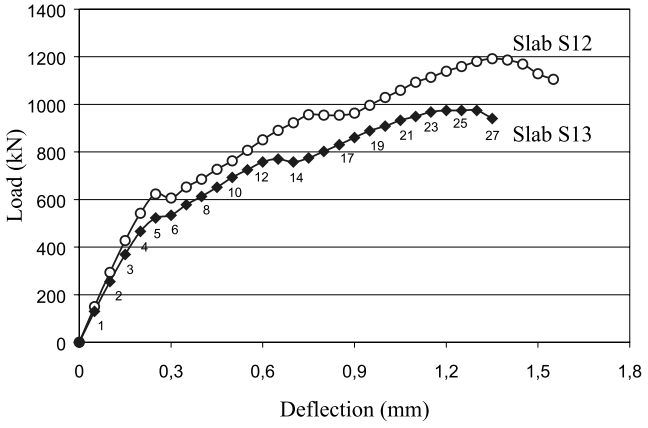

Fig. 8. Computed load–deflection curves of slabs S12 and S13.

ultimate loads were slightly larger than those observed in the tests. Slabs 12 and 13 failed at 1049 and 803 kN, respectively. The computed ultimate loads are 1192 and 975 kN, respectively. The load–deflection curves of the circular slabs were not recorded in the test. However, the deflection at ultimate load of a tested equivalent square slab, with corresponding material properties and with the same depth as slab S12, was approximately equal to the computed deflection at ultimate load of slab S12, i.e., 1.3 mm.

In the FE-analyses, the reinforcement never reaches the yield stress, which is in accordance with observations made in the tests of slabs S12 and S13.

The load–deflection curves in Fig. 8 can each be divided into four phases. The numbers of the deformation steps of slab S13 are given next to the curve of the slab. From step 0 to step 2 the slab is uncracked. Hence, the slab is in a linear-elastic phase. At step 2, the first flexural cracks appear and the slab runs into a flexural deformation phase.

At step 5, the first inclined shear cracks appear, see Fig. 9(a), and the slab runs into a shear deformation phase. At step 14, the compression stresses at the bottom of the slab reach the compressive strength of concrete, see Fig. 9(b), and the concrete starts to crush and soften in compression. The element in which the crushing criterion is reached is marked light grey in Fig. 9. Simultaneously, a crack runs through the same element and the band of shear cracks have now propagated through the complete depth of the slab.

One would assume that the ultimate load would be reached now. However, a new phase is entered where the load still increases as the deformation is increased. The stresses are redistributed through a compression strut. As the load increases, the crushing criterion is reached in the elements above the first one. Eventually, crushing is reached throughout the width of the compression strut and the concrete has softened in compression down to zero stress. At this point, the ultimate load has been reached and the column footing has failed in punching shear, see Fig. 9(c).

5. Parametric study

In order to investigate the influence of various parameters on the punching shear behaviour of column footings, a parametric study was conducted where the FE-analysis of slab S13 was repeated with increased values of the parameters.

Fig. 10 shows the influence of the slenderness, i.e., the shear-span to depth ratio *a*/*d*, on the load–deflection

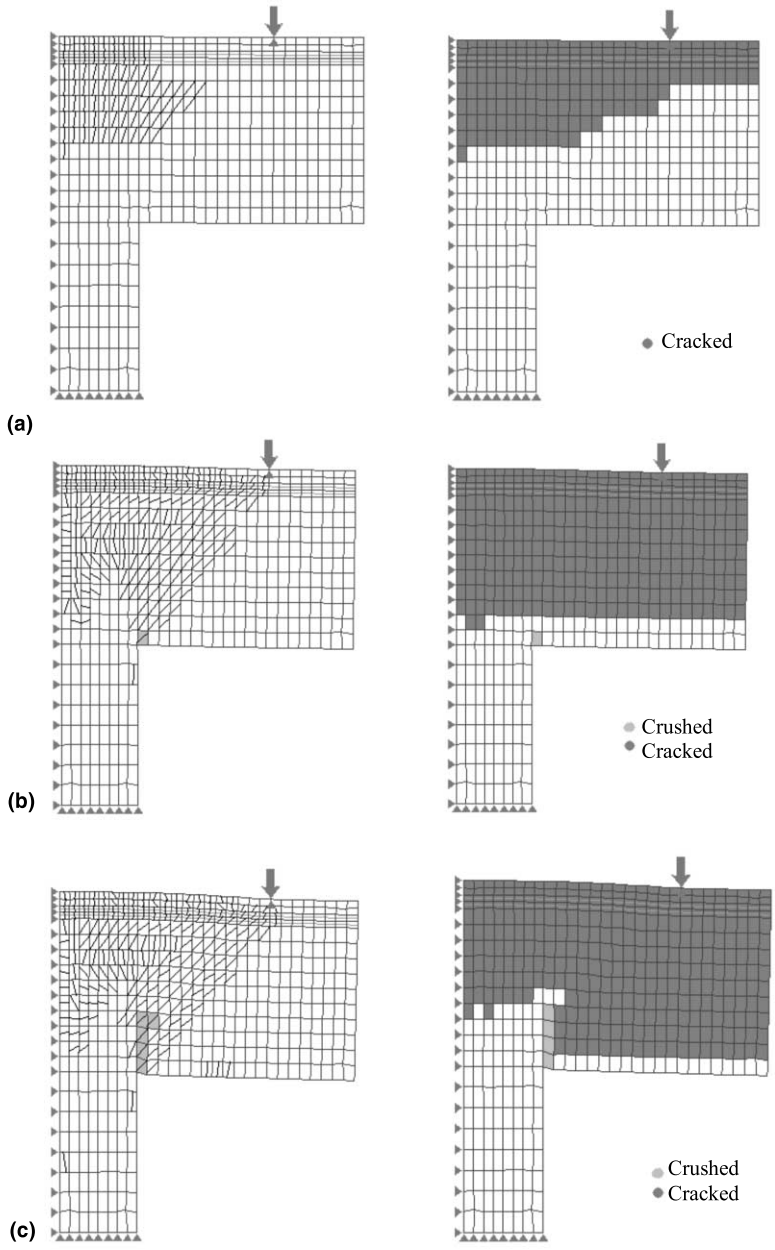

Fig. 9. Computed crack and crush patterns (left) tangential cracks (right) radial cracks. (a) Deformation step 5. (b) Deformation step 14. (c) Deformation step 27.

curve. The ultimate load decreases and the deflection at ultimate load increases as the slenderness is increased. It appears that the last phase of the curve, where the compression strut is crushed, is missing for the slabs with higher slenderness. Hence, the failure mechanism is changed as the slenderness is increased.

Table 2 shows a summary of the parametric study by giving the influence of various parameters on the computed ultimate load.

The compressive strength of concrete appears to have the largest influence on the ultimate load. In previous FE-analyses on more slender slabs, i.e., with higher

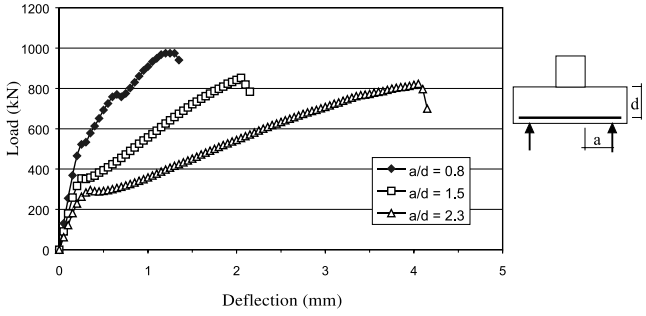

Fig. 10. Computed load–deflection curves of slabs with different slenderness a/d.

Table 2
Influence of parameters on the computed ultimate load P_u

Slenderness			
a/d	0.8	1.5 (+ 88%)	2.3 (+188%)
P_u (kN)	975	853 (−13%)	822 (−16%)
Concrete compressive strength			
f_{cc} (MPa)	21.0	29.5 (+40%)	38.0 (+81%)
P_u (kN)	975	1190 (+22%)	1404 (+44%)
Concrete tensile strength			
f_{ct} (MPa)	2.0	2.5 (+25%)	3.0 (+50%)
P_u (kN)	975	961 (−1%)	982 (+1%)
$P_{crack\text{-}through}$ (kN)	770	893 (+16%)	975 (+27%)
Fracture energy			
G_f (N/m)	98	123 (+26%)	145 (+48%)
P_u (kN)	975	955 (−2%)	959 (−2%)

values of a/d [6,7], the compressive strength of concrete, ranging from 60 to 120 MPa, did hardly have any influence on the ultimate load at all. Hence, the compressive strength seems to be more important for slabs with low a/d-ratios, which is also supported by the type of failure mechanism described in Section 4.

The previous studies [6,7] indicated that the tensile strength and the fracture energy of concrete had a significant influence on the punching shear strength of slender slabs. However, in the present study the tensile strength and the fracture energy of concrete appear to have no significant influence on the ultimate strength. However, the load at which the shear crack runs through the slab, $P_{crack\text{-}through}$, increases with increasing tensile strength of concrete.

6. Conclusions

The comparison between the FE-analyses and the tests shows good conformity. Furthermore, and even more important, the numerical results give valuable information on the mechanism of concrete cracking and stress distribution within a slab prior and during a punching shear failure. The failure mechanism at ultimate load of the column footings in this investigation is governed by crushing of the compression strut. The parametric study showed that the compressive strength of concrete has a higher influence on the load capacity of column footings than previously shown in studies with slender slabs.

The results from this investigation could preferably be used for the development of new design methods, or further development of current design methods, in order to make them valid for slabs with low shear-span to depth ratios also. Hereby, the new or further developed design methods should be based on mechanical models rather than on empirically derived formulas.

Further experimental research is also needed. The column footings tested hitherto were usually much smaller than real footings, found in e.g., bridges. In order to check the size effect, test on larger slabs with small shear-span to depth ratios are of great interest. As high strength concrete is available now, and tests on column footings indicate a strong influence of the compressive strength, high strength concrete footings should also be tested.

References

[1] Dieterle H. Zur Bemessung von Fundamentplatten ohne Schubbewehrung. Beton-und Stahlbetonbau 1978;73(H. 2):29–37 (in German).
[2] Hallgren M, Kinnunen S, Nylander B. Punching Shear Tests on Column Footings. Nordic Concrete Research, Publication No 21, 1. 1998. p. 1–22.
[3] Bjerke M. Icke-linjära finita-elemetanalyser av grundplattor belastade till genomstansning. M.Sc. thesis No. 124, Concrete Structures, Department of Structural Engineering, Royal Institute of Technology, Stockholm, 1999 (in Swedish).
[4] Cervenka Consulting. SBETAX, Nonlinear Axi-symmetric Finite Element Analysis of Concrete Structures. Program manual, Prague, 1997.
[5] Cervenka V, Pukl R. SBETA, version 11 Program documentation. Prague: Cervenka Consulting; 1996.
[6] Hallgren M. Punching shear capacity of reinforced high strength concrete slabs. Ph.D. thesis, Bulletin No. 23, Department of Structural Engineering, Royal Institute of Technology, Stockholm, 1996.
[7] Menetrey P. Numerical analysis of punching failure in reinforced concrete structures. Ph.D. thesis, Thése No. 1279, Département de Génie Civil, École Polytechnique Féderal de Lausanne, Lausanne, 1994.
[8] MC90, "CEB-FIP Model Code 90", Bullein dínformation No. 213/214, CEB, Lausanne, 1993.